

See discussions, stats, and author profiles for this publication at: <https://www.researchgate.net/publication/231630424>

# Convergence of the Electrostatic Interaction Based on Topological Atoms

ARTICLE *in* THE JOURNAL OF PHYSICAL CHEMISTRY A · AUGUST 2001

Impact Factor: 2.69 · DOI: 10.1021/jp011511q

---

CITATIONS

100

---

READS

20

3 AUTHORS, INCLUDING:



**Paul L A Popelier**

The University of Manchester

**190** PUBLICATIONS **7,122** CITATIONS

SEE PROFILE



**L. Joubert**

Université de Rouen

**82** PUBLICATIONS **1,082** CITATIONS

SEE PROFILE

# Convergence of the Electrostatic Interaction Based on Topological Atoms

P. L. A. Popelier,\* L. Joubert, and D. S. Kosov†

Department of Chemistry, UMIST, Manchester, M60 1QD, England

Received: April 19, 2001; In Final Form: June 5, 2001

An atom–atom partitioning of the electrostatic energy between unperturbed molecules is proposed on the basis of the topology of the electron density. Atom–atom contributions to the electrostatic energy are computed exactly, i.e., via a novel six-dimensional integration over two atomic basins, and by means of the spherical tensor multipole expansion, up to total interaction rank  $L = l_A + l_B + 1 = 6$ . The convergence behavior of the topological multipole expansion is compared with that using distributed multipole analysis (DMA) multipole moments for a set of van der Waals complexes at the B3LYP/6-311+G(2d,p) level. Within the context of the Buckingham–Fowler model it is shown that the topological and DMA multipole moments converge to a very similar interaction energy and geometry (average absolute discrepancy of 1.3 kJ/mol and 1.3°, respectively) and are both in good to excellent agreement with supermolecule calculations.

## 1. Introduction

It is well-known that the electrostatic energy often dominates the interaction between molecules, especially polar ones. The popular Buckingham–Fowler model<sup>1,2</sup> benefits from this fact as it successfully predicts the qualitative angular features of hydrogen-bonded van der Waals complexes simply by using an electrostatic and a simple repulsion term. In this model the electrostatic component consists of interaction terms between multipole moments provided by Stone's distributed multipole analysis (DMA),<sup>3</sup> while the short-range repulsion force is simulated by hard spheres placed on the atomic centers. The DMA method has been used for many systems<sup>4,5</sup> that benefit from an anisotropic description beyond point charges. Moreover, qualitative chemical insight into the nature of the charge distribution can be obtained from a distributed model. It is here that an alternative to DMA emerges in the form of the topological analysis of the electron density or the theory of "Atoms in Molecules" (AIM).<sup>6–8</sup>

Cooper and Stutchbury<sup>9</sup> have successfully used the topological partitioning method to study a series of van der Waals complexes. However, their work was criticized later<sup>10</sup> on the grounds of poor convergence of the multipole expansion of the electrostatic interaction. Because the higher atomic moments are much larger than the overall molecular moments, it was claimed<sup>10</sup> that "any form of distributed multipole analysis that rests on a physical division of space into disjoint regions is unlikely to be useful". The main purpose of this paper is to scrutinize this statement and assess the convergence properties of AIM multipole moments more rigorously. We show that although the AIM multipole expansion converges more slowly than the DMA expansion, it is nonetheless useful (despite its computational expense) since both expansions converge to the same answer when high rank terms are included. This direct and explicit comparison between DMA and AIM has never been made before. Moreover the comparison is made both in terms

of geometries and interaction energies, supplemented with supermolecule calculations. Further novelties include the high multipolar rank of interaction ( $L = l_A + l_B + 1 = 6$ , see Section 2, e.g., dipole–hexadecapole) and the use of analytical first and second derivatives of the interaction energy with respect to rigid body coordinates<sup>11</sup> combined with the eigenvector following method<sup>12</sup> to explore the potential energy surfaces. Finally, we are presenting for the first time the exact electrostatic interaction between topological atoms.

We have looked at a range of van der Waals complexes containing HF including (HF)<sub>2</sub>, HF⋯N<sub>2</sub>O, HF⋯CO<sub>2</sub>, HF⋯H<sub>2</sub>O, HF⋯NH<sub>3</sub>, HF⋯HCN, HF⋯H<sub>2</sub>CO, and the water dimer, (H<sub>2</sub>O)<sub>2</sub>.

## 2. Atom–Atom Electrostatic Interaction Energy

The first-order term within the long-range perturbation theory<sup>13</sup> corresponds to the electrostatic interaction energy between molecules  $M_A$  and  $M_B$ , which is defined as

$$E_{\text{elec}}(M_A, M_B) = \int d\mathbf{r}_1 \int d\mathbf{r}_2 \frac{\rho_{\text{tot}}(M_A; \mathbf{r}_1) \rho_{\text{tot}}(M_B; \mathbf{r}_2)}{|\mathbf{r}_1 - \mathbf{r}_2|} \quad (1)$$

where the total ground-state charge density of molecule  $M$  is given by

$$\rho_{\text{tot}}(M; \mathbf{r}) = \sum_{i \in M} Z_i \delta(\mathbf{r} - \mathbf{R}_i) - \rho(M; \mathbf{r}) \quad (2)$$

In eq 2  $\rho(M; \mathbf{r})$  is the ground-state electron density of an unperturbed molecule  $M$  and the index  $i$  runs over all nuclei in molecule  $M$ . Equation 1 expresses the exact classical interaction energy of two molecular charge distributions in a form that does not depend on the multipole expansion. Although each molecular charge distribution is described in its own coordinate system, the position of the two molecules with respect to each other must be known. Only when the relationship between  $\mathbf{r}_1$  and  $\mathbf{r}_2$  is known can the interelectron distance  $|\mathbf{r}_1 - \mathbf{r}_2|$  and the six-dimensional integral be computed.

The volume integrals in eq 1 extend over all space. To partition  $E_{\text{elec}}(M_A, M_B)$  in terms of atom–atom interactions, we

\* Corresponding author. Fax: +44-161-200 4559. E-mail: pla@umist.ac.uk. <http://www.ch.umist.ac.uk/popelier.htm>.

† Present address: Institut für Physikalische und Theoretische Chemie, J. W. Goethe Universität, Marie-Curie Str. 11, 60439 Frankfurt/Main, Germany.

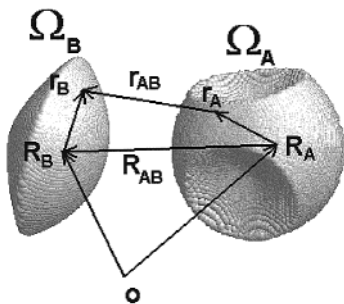


**Figure 1.** Coordinate system used in the description of the electrostatic interaction between two atomic basins  $\Omega_A$  and  $\Omega_B$ . The vector  $\mathbf{R}_A$  ( $\mathbf{R}_B$ ) is the position vector of the nucleus A(B), both referred to the global origin  $\mathbf{o}$ . The vector  $\mathbf{R}_{AB} = \mathbf{R}_B - \mathbf{R}_A$  is the internuclear vector and  $\mathbf{r}_A$  ( $\mathbf{r}_B$ ) marks the position of an infinitesimal charge element in  $\Omega_A$  ( $\Omega_B$ ) with respect to the nuclear origin  $\mathbf{R}_A$  ( $\mathbf{R}_B$ ). The vector  $\mathbf{r}_{AB} = (\mathbf{R}_B + \mathbf{r}_B) - (\mathbf{R}_A + \mathbf{r}_A) = \mathbf{R}_{AB} - (\mathbf{r}_A - \mathbf{r}_B)$  measures the distance between two charge elements (with respect to the global origin).

use the theory of AIM. In this theory an atom is defined as a bounded portion of real space determined by the gradient vector field of  $\rho(\mathbf{r})$ . The gradient of the electron density,  $\nabla\rho(\mathbf{r})$  traces gradient paths, which are paths of steepest ascent through  $\rho(\mathbf{r})$ . An infinite number of gradient paths originating at infinity terminate at a maximum in  $\rho(\mathbf{r})$ , which practically coincides with a nuclear position. Such a collection of gradient paths occupies a portion of space called an atomic basin, denoted by  $\Omega$ . An atomic basin together with its nucleus constitutes an atom. This procedure divides space up into nonoverlapping atoms in an exhaustive manner. Atomic properties are defined as volume integrals over the atomic basins; for example, the population associated with an atom is the volume integral of  $\rho(\mathbf{r})$  over the basin.

The exact electrostatic energy between two atoms  $A$  and  $B$ , belonging to molecule  $M_A$  and  $M_B$ , respectively, is then defined as

$$E_{\text{elec}}(A,B) = \int_{\Omega_A} d\mathbf{r}_1 \int_{\Omega_B} d\mathbf{r}_2 \frac{\rho_{\text{tot}}(M_A;\mathbf{r}_1)\rho_{\text{tot}}(M_B;\mathbf{r}_2)}{|\mathbf{r}_1 - \mathbf{r}_2|} \quad (3)$$

In view of the additivity of AIM atomic properties the electrostatic interaction energy between two molecules is simply:

$$E_{\text{elec}}(M_A, M_B) = \frac{1}{2} \sum_A \sum_{B \neq A} E_{\text{elec}}(A,B) \quad (4)$$

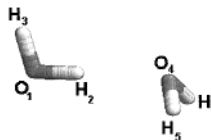
It is possible to compute  $E_{\text{elec}}(A,B)$  directly without recourse to a multipole expansion, in which case we refer to its value as being “exact”. However, this does not mean that the six-dimensional integral in eq 3 is calculated analytically, because we use a quadrature procedure. Integration by quadrature over a single atomic basin is well-documented,<sup>14,15</sup> but here we report a double integration, i.e., a simultaneous quadrature over two atomic basins.

In the appendix we show that eq 3 can be re-expressed in terms of a multipole expansion as follows:

$$E_{\text{elec}}(A,B) = \sum_{l_A l_B k_A k_B} T_{l_A l_B k_A k_B}(\mathbf{R}_{AB}) Q_{l_A k_A}(\Omega_A) Q_{l_B k_B}(\Omega_B) \quad (5)$$

where  $T_{l_A l_B k_A k_B}$  is a purely geometric interaction tensor, the intersite-vector  $\mathbf{R}_{AB} = \mathbf{R}_B - \mathbf{R}_A$  (see Figure 1), and  $Q_{lk}$  are the  $2l+1$  multipole moments of rank  $l$  with respect to the local frame centered on each nucleus.

**TABLE 1: Comparison<sup>a</sup> between DMA and AIM in Terms of (a) the Total Electrostatic Interaction Energy  $E_{\text{elec}}(\text{H}_2\text{O}, \text{H}_2\text{O})$  (kJ/mol), (b) the AIM Atom–Atom Partitioning of the Electrostatic Energy,  $E_{\text{elec}}(A,B)$  (kJ/mol), as a Function of the Multipolar Expansion Rank  $L$ , and (c) the Geometry (Distances in Å and Angles in deg) between the Monomers in  $(\text{H}_2\text{O})_2$**

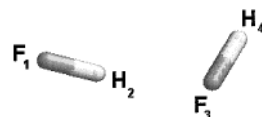


(a)			
	L	AIM <sup>c</sup>	DMA <sup>c</sup>
	1	−37.1	−5.7
	2	−12.4	−14.0
	3	−24.7	−21.0
	4	−21.3	−23.5
	5	−24.6	−24.9
	6	−25.7	−24.7
	exact	−30.5	
(b)			
AIM	L	O <sub>4</sub>	H <sub>5</sub>
O <sub>1</sub>	1	533.6	−236.3
	2	535.1	−244.7
	3	536.1	−242.2
	4	532.1	−241.4
	5	529.8	−241.2
	6	529.7	−241.1
	exact	529.0	−241.2
H <sub>2</sub>	1	−388.8	160.0
	2	−351.6	157.2
	3	−365.9	156.2
	4	−361.3	156.6
	5	−362.7	156.6
	6	−364.0	156.7
	exact	−367.8	156.7
H <sub>3</sub>	1	−235.0	102.8
	2	−236.9	108.0
	3	−239.0	108.1
	4	−238.9	108.1
	5	238.9	108.1
	6	−238.9	108.1
	exact	−238.9	108.1
(c)			
coordinate <sup>b</sup>	AIM	DMA	supermolecule
$R(\text{O}_4\text{--H}_2)$	2.104	2.107	1.943
$\angle(\text{O}_4\text{--H}_2\text{--O}_1)$	176.3	175.6	174.4
$\angle(\text{H}_5\text{--O}_4\text{--H}_2)$	106.9	109.3	112.2

<sup>a</sup> The interaction between H<sub>6</sub> and other atoms is identical to that of H<sub>5</sub> because of the mirror plane. <sup>b</sup> Corresponding to a minimization of the total interaction energy including the short-range repulsion (as in Tables 2–8). <sup>c</sup> Energies correspond to the respective equilibrium geometries (as in Tables 2–8).

We should keep in mind that even when the multipolar expansion converges the electrostatic energy thus obtained is only an approximation<sup>16</sup> to the true electrostatic energy obtained by 6D integration (see eq 3). The remaining difference is called the penetration energy<sup>13</sup> and arises at short range when the charge clouds of  $\rho_A$  and  $\rho_B$  sufficiently overlap. In contrast to previous work<sup>17</sup> where the atoms were taken from supermolecules, the atoms in this work do overlap because they were taken from separate isolated monomers and superimposed according to the geometry of the van der Waals complex. The penetration effect results from the fact that nuclei on one molecule will no longer be shielded by that molecule’s own

**TABLE 2: Comparison between DMA and AIM in Terms of (a) the Total Electrostatic Interaction Energy  $E_{\text{elec}}(\text{HF}, \text{HF})$  (kJ/mol), (b) the AIM Atom–Atom Partitioning of the Electrostatic Energy,  $E_{\text{elec}}(\text{A}, \text{B})$ , as a Function of the Multipolar Expansion Rank  $L$ , and (c) the Geometry (distances in Å and Angles in deg)**



(a)			
L	AIM	DMA	
1	−38.4	−12.0	
2	−11.7	−14.7	
3	−17.3	−18.2	
4	−16.9	−17.9	
5	−18.4	−17.8	
6	−18.4	−18.1	
<b>exact</b>	<b>−20.6</b>		

(b)			
	L	F <sub>3</sub>	H <sub>4</sub>
F <sub>1</sub>	1	230.3	−198.5
	2	241.9	−215.4
	3	238.9	−215.0
	4	238.5	−214.7
	5	238.0	−214.6
	6	238.1	−214.5
	<b>exact</b>	<b>237.8</b>	<b>−214.5</b>
H <sub>2</sub>	1	−332.4	262.2
	2	−298.7	260.6
	3	−300.8	259.6
	4	−300.4	259.7
	5	−301.5	259.6
	6	−301.6	259.7
	<b>exact</b>	<b>−303.4</b>	<b>259.5</b>

(c)			
coordinate	AIM	DMA	supermolecule
$R(\text{H}_2\text{--F}_3)$	2.061	2.065	1.822
$\angle(\text{H}_2\text{--F}_3\text{--H}_4)$	116.9	119.2	115.6
$\angle(\text{F}_1\text{--H}_2\text{--F}_3)$	169.6	168.2	166.2
$\angle(\text{H}_2\text{--F}_1\text{--F}_3)$	7.2	8.2	9.2
$\angle(\text{F}_1\text{--F}_3\text{--H}_4)$	113.7	115.6	110.9

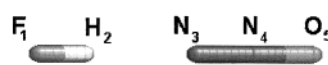
electron density but will also experience an attraction for the electron density of the other molecule. The penetration energy is a negative correction to the interaction energy, and its treatment in the context of the electrostatic penetration has only recently been explored.<sup>18</sup>

### 3. Computational Methods

Three computer programs were used in our calculations. First, the geometry optimizations and wave functions of isolated molecules and molecular complexes were obtained by the program GAUSSIAN98.<sup>19</sup> We used the B3LYP/6-311+G(2d,p) level of theory<sup>20,21</sup> for both the geometry optimizations and the wave functions because it has proven to be a good compromise between accuracy and computational cost.<sup>22,23</sup>

Spherical tensor AIM multipole moments<sup>14,15</sup> were computed by using a local version of the program MORPHY01.<sup>24</sup> MORPHY also generated the partitioned electrostatic energy defined in eq 3 via direct integration, i.e., without multipolar expansion. The atomic basin was capped by the  $\rho = 10^{-7}$  au isodensity envelope. The integration errors measured via  $L(\Omega)^{25}$  for single-basin 3D integrations were all below  $1 \times 10^{-4}$  au. For the two-basin 6D integrations, required to evaluate

**TABLE 3: Comparison between DMA and AIM in Terms of (a) the Total Electrostatic Interaction Energy  $E_{\text{elec}}(\text{HF}, \text{N}_2\text{O})$  (kJ/mol), (b) the AIM Atom–atom Partitioning of the Electrostatic Energy,  $E_{\text{elec}}(\text{A}, \text{B})$  (kJ/mol), as a Function of the Multipolar Expansion Rank  $L$ , and (c) the Geometry (Distances in Å and Angles in deg) between the Monomers in  $\text{HF}\cdots\text{N}_2\text{O}$**



(a)			
L	AIM	DMA	
1	17.0	−4.5	
2	−43.4	−10.3	
3	1.4	−11.0	
4	−8.4	−11.5	
5	−12.8	−10.3	
6	−10.6	−10.6	
<b>exact</b>	<b>−12.7</b>		

(b)				
	L	N <sub>3</sub>	N <sub>4</sub>	O <sub>5</sub>
F <sub>1</sub>	1	−33.0	−55.0	61.7
	2	11.4	−45.9	58.6
	3	9.3	−48.9	55.8
	4	6.1	−50.2	55.4
	5	7.2	−50.0	55.5
	6	7.0	−49.9	55.5
	<b>exact</b>	<b>6.4</b>	<b>−49.9</b>	<b>55.5</b>
H <sub>2</sub>	1	47.3	70.6	−74.5
	2	−51.4	48.0	−64.1
	3	−13.2	59.3	−60.8
	4	−18.1	59.2	−60.9
	5	−23.0	58.6	−61.0
	6	−20.6	58.6	−61.0
	<b>exact</b>	<b>−22.4</b>	<b>58.7</b>	<b>−61.0</b>

(c)			
coordinate	AIM	DMA	supermolecule
$R(\text{H}_2\text{--N}_3)$	2.142	2.142	2.000
$\angle(\text{H}_2\text{--N}_3\text{--N}_4)$	180.0	180.0	180.0

$E_{\text{elec}}(\text{A}, \text{B})$ , several calculations were repeated with different quadrature grids to check the stability of the direct integration.<sup>17</sup> Deviations are on the order of 0.1 kJ/mol, depending on the size and distribution of quadrature points in the integration grid. For example, the computation of  $E_{\text{elec}}(\text{N}_3, \text{F}_1)$  in  $\text{HF}\cdots\text{NH}_3$  by two different quadrature grids of approximately two and one million points yields an energy of 360.4 and 360.5 kJ/mol, respectively.

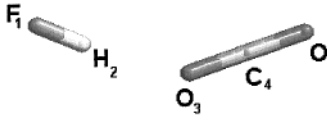
Finally the program ORIENT3.2j<sup>26</sup> was used to evaluate eq 12, which has currently been implemented up to  $L = l_A + l_B + 1 = 6$  or  $\mathbf{R}_{\text{AB}}^{-6}$ . ORIENT is designed for the anisotropic interaction between multipoles moments expressed with respect to *local* axis systems that have an arbitrary relative orientation, for example, between rigid monomers. In this work we make full use of the capability of ORIENT.

The values for the pseudo-hard-sphere (i.e., slightly softened) van der Waals radii<sup>27</sup> are 1.47 Å for F, 1.55 Å for N, 1.52 Å for O and 1.70 Å for C. Hydrogen is not assigned a radius. In the work of Buckingham and Fowler<sup>2</sup> (and also of Cooper and Stutchbury<sup>9</sup>) slightly different values were used.<sup>28</sup>

### 4. Results and Discussion

The results for eight van der Waals systems are given in Tables 1–8, each of which contains a labeling diagram of the corresponding equilibrium geometry. Each table consists of three parts: (a) the convergence behavior as a function of  $L$  of the

TABLE 4: Comparison between DMA and AIM in Terms of (a) the Total Electrostatic Interaction Energy  $E_{\text{elec}}(\text{HF}, \text{CO}_2)$  (kJ/mol), (b) the AIM Atom–Atom Partitioning of the Electrostatic Energy,  $E_{\text{elec}}(\text{A}, \text{B})$  (kJ/mol), as a Function of the Multipolar Expansion Rank  $L$ , and (c) the Geometry (Distances in Å and Angles in deg) between the Monomers in  $\text{HF} \cdots \text{CO}_2$



(a)				
		AIM	DMA	
	1	−44.2	−12.3	
	2	−6.1	−11.5	
	3	−5.1	−12.0	
	4	−9.6	−10.3	
	5	−10.1	−9.4	
	6	−10.3	−9.7	
	<b>exact</b>	<b>−11.6</b>		

	L	O <sub>3</sub>	C <sub>4</sub>	O <sub>5</sub>
F <sub>1</sub>	1	345.6	−522.2	206.7
	2	348.4	−554.2	227.3
	3	339.2	−555.1	227.2
	4	338.8	−555.4	226.8
	5	338.5	−554.9	226.7
	6	338.7	−554.8	226.7
	<b>exact</b>	<b>338.5</b>	<b>−554.8</b>	<b>226.7</b>
H <sub>2</sub>	1	−496.3	670.6	−248.6
	2	−418.9	651.1	−259.8
	3	−416.7	657.9	−257.6
	4	−419.9	657.3	−257.2
	5	−420.1	657.1	−257.3
	6	−420.7	657.2	−257.3
	<b>exact</b>	<b>−421.9</b>	<b>657.2</b>	<b>−257.3</b>

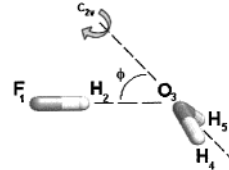
	coordinate	AIM	DMA	supermolecule
	$R(\text{O}_3\text{--H}_2)$	2.122	2.117	1.959
	$\angle(\text{H}_2\text{--O}_3\text{--C}_4)$	143.4	180.0	144.6
	$\angle(\text{F}_1\text{--H}_2\text{--O}_3)$	174.3	180.0	172.5

total electrostatic interaction energy between the two monomers, denoted by  $E_{\text{elec}}(M_A, M_B)$  (see eq 4), (b) a complete atom–atom breakdown of the electrostatic energy according to AIM, given by individual contributions  $E_{\text{elec}}(\text{A}, \text{B})$  (see eq 3), and (c) a comparison between selected geometrical parameters produced by the DMA and AIM model and an ab initio calculation of the complex.

From part a in Tables 1–8 it is clear that for a multipole expansion up to  $L = 6$  the values of  $E_{\text{elec}}(M_A, M_B)$  are very similar, showing an average absolute deviation of 1.3 kJ/mol, with a minimum value <0.1 kJ/mol and a maximum value of 3.9 kJ/mol. The exact energy, computed via 6D integration, is always lower than AIM's  $L = 6$  result, by an average value of 2.9 kJ/mol, ranging between 0.7 and 6.6 kJ/mol. The corresponding average deviation for DMA is 2.8 kJ/mol, ranging between 1.3 and 5.8 kJ/mol. In light of the discussion on the penetration energy in section 2, we do expect the exact electrostatic energy to be lower than the best possible converged multipole expansion. From these comparisons we conclude that DMA and AIM both tend to converge to the same total interaction energy.

From part b, we see that  $E_{\text{elec}}(\text{A}, \text{B})$  is typically about an order of magnitude larger than the total monomer–monomer interac-

TABLE 5: Comparison<sup>a</sup> between DMA and AIM in Terms of (a) the Total Electrostatic Interaction Energy  $E_{\text{elec}}(\text{HF}, \text{H}_2\text{O})$  (kJ/mol), (b) the AIM Atom–Atom Partitioning of the Electrostatic Energy,  $E_{\text{elec}}(\text{A}, \text{B})$  (kJ/mol), as a Function of the Multipolar Expansion Rank  $L$ , and (c) the Geometry (Distances in Å and Angles in deg) between the Monomers in  $\text{HF} \cdots \text{H}_2\text{O}$



(a)			
		AIM	DMA
	1	−55.1	−12.0
	2	−21.2	−22.6
	3	−34.8	−29.8
	4	−28.7	−32.1
	5	−32.4	−32.5
	6	−32.6	−32.4
	<b>exact</b>	<b>−35.6</b>	

	L	O <sub>3</sub>	H <sub>4</sub>
F <sub>1</sub>	1	351.4	−150.9
	2	375.0	−165.9
	3	375.2	−165.7
	4	374.5	−165.5
	5	373.3	−165.3
	6	373.2	−165.3
	<b>exact</b>	<b>371.8</b>	<b>−165.3</b>
H <sub>2</sub>	1	−506.5	200.9
	2	−470.7	203.1
	3	−482.4	201.9
	4	−476.3	202.1
	5	−479.0	202.0
	6	−479.4	202.1
	<b>exact</b>	<b>−481.0</b>	<b>202.1</b>

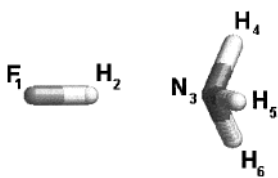
	coordinate	AIM	DMA	supermolecule
	$R(\text{O}_3\text{--H}_2)$	2.090	2.091	1.687
	$\angle(\text{O}_3\text{--H}_2\text{--F}_1)$	175.2	174.3	176.6
	$\angle(\text{H}_2\text{--O}_3\text{--H}_4)$	114.2	114.8	113.7
	$\phi$	47.7	46.3	47.5

<sup>a</sup> The interaction between H<sub>5</sub> and the other atoms is identical to that of H<sub>4</sub> because of the mirror plane.

tion energy, although we find values as low as 7 kJ/mol in  $\text{HF} \cdots \text{N}_2\text{O}$ . In all systems the hydrogen-bonded atom pair (e.g.,  $E_{\text{elec}}(\text{H}_2, \text{F}_3)$  in  $(\text{HF})_2$ ) has a negative electrostatic energy (for  $L = 6$ ), which is typically more than 10 times larger than the total interaction energy of the complex. This observation emphasizes that the total interaction energy, which would be ascribed to hydrogen bond formation in all eight complexes, is in fact due to cancellation of large atom–atom contributions. For example, in  $(\text{HF})_2$ ,  $E_{\text{elec}}(\text{HF}, \text{HF}) = E_{\text{elec}}(\text{F}_1, \text{F}_3) + E_{\text{elec}}(\text{F}_1, \text{H}_4) + E_{\text{elec}}(\text{H}_2, \text{F}_3) + E_{\text{elec}}(\text{H}_2, \text{H}_4) = -20.6 = 237.8 - 214.5 - 303.4 + 259.5$  kJ/mol. The intermolecular interaction observed at  $L = 1$  warns that AIM monopoles must not be misunderstood to be able to compete with point charges designed to model electrostatic interactions.<sup>29</sup> The convergence of  $E_{\text{elec}}(\text{A}, \text{B})$  improves as the atoms are further away from each other. The worse convergence occurs for the hydrogen-bonded atoms where  $E_{\text{elec}}(\text{A}, \text{B}, \text{exact}) - E_{\text{elec}}(\text{A}, \text{B}, L = 6)$  ranges from −3.8 to −1.2 kJ/mol (average = −2.0 kJ/mol). Beside impairing the multipole



TABLE 6: Comparison<sup>a</sup> between DMA and AIM in Terms of (a) the Total Electrostatic Interaction Energy  $E_{\text{elec}}(\text{HF}\cdots\text{NH}_3)$  (kJ/mol), (b) the AIM Atom–Atom Partitioning of the Electrostatic Energy,  $E_{\text{elec}}(\text{A},\text{B})$  (kJ/mol), as a Function of the Multipolar Expansion Rank  $L$ , and (c) the Geometry (Distances in Å and Angles in deg) between the Monomers in  $\text{HF}\cdots\text{NH}_3$



(a)			
	AIM	DMA	
1	-48.6	-8.3	
2	-30.0	-23.4	
3	-60.7	-40.9	
4	-39.3	-45.7	
5	-49.0	-50.2	
6	-45.0	-48.1	
<b>exact</b>	<b>-51.6</b>		

(b)			
	$L$	$\text{N}_3$	$\text{H}_4$
$\text{F}_1$	1	315.8	-90.3
	2	354.1	-102.0
	3	368.2	-102.2
	4	367.5	-102.1
	5	365.5	-102.0
	6	365.0	-101.9
	<b>exact</b>	<b>360.4</b>	<b>-101.9</b>
$\text{H}_2$	1	-454.0	120.2
	2	-458.2	126.7
	3	-498.6	125.4
	4	-477.8	125.7
	5	-485.3	125.6
	6	-481.3	125.7
	<b>exact</b>	<b>-483.4</b>	<b>125.7</b>

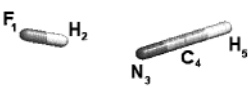
(c)			
coordinate	AIM	DMA	supermolecule
$R(\text{N}_3\text{--H}_2)$	2.112	2.109	1.664
$\angle(\text{N}_3\text{--H}_2\text{--F}_1)$	180.0	180.0	180.0

<sup>a</sup> The interaction between  $\text{H}_5$  ( $\text{H}_6$ ) and other atoms is identical to that of  $\text{H}_4$  because of the 3-fold axis.

convergence, such proximity also introduces a nonnegligible penetration energy.

Part c shows that the supermolecular geometry is in good to excellent agreement with experiment. In total there are 18 angles of which only 3 show large deviations between AIM and DMA. The average absolute difference of the remaining 15 angles is only  $1.3^\circ$ , ranging between  $0.2^\circ$  and  $2.6^\circ$ . The three excluded angles occur in the complexes  $\text{HF}\cdots\text{CO}_2$  and  $\text{HF}\cdots\text{HCN}$ . Using our basis set, supermolecule calculations predicts that, at both the B3LYP and the MP2 level, the most stable minimum of the  $\text{HF}\cdots\text{CO}_2$  complex is bent by 0.4 and 0.3 kJ/mol respectively, where the linear structure is a transition state. At  $L = 6$ , DMA wrongly predicts a linear structure, while AIM generates a structure that deviates by only a few degrees from the supermolecular values. On the other hand, in the  $\text{HF}\cdots\text{HCN}$  complex, DMA correctly predicts a linear geometry (as opposed to AIM), but the difference between the linear and bent minima is only 0.8 kJ/mol (B3LYP) or 0.2 kJ/mol (MP2). These observations lead to the important conclusion that DMA and

TABLE 7: Comparison<sup>a</sup> between DMA and AIM in Terms of (a) the Total Electrostatic Energy  $E_{\text{elec}}(\text{HF}\cdots\text{HCN})$  (kJ/mol), (b) the AIM Atom–Atom Partitioning of the Electrostatic Energy,  $E_{\text{elec}}(\text{A},\text{B})$ , as a Function of the Multipolar Expansion Rank  $L$ , and (c) the Geometry (Distances in Å and Angles in deg) between the Monomers in  $\text{HF}\cdots\text{HCN}$



(a)				
		AIM	DMA	
1		-80.6	-26.4	
2		-12.3	-19.9	
3		-15.3	-28.6	
4		-26.9	-27.2	
5		-25.6	-28.1	
6		-25.0	-28.9	
<b>exact</b>		<b>-27.6</b>		

(b)				
	$L$	$\text{N}_3$	$\text{C}_4$	$\text{H}_5$
$\text{F}_1$	1	336.6	-200.8	-39.6
	2	344.7	-241.2	-43.7
	3	335.8	-248.6	-44.2
	4	336.5	-248.2	-44.1
	5	336.7	-247.6	-44.1
	6	336.6	-247.4	-44.1
	<b>exact</b>	<b>335.6</b>	<b>-247.4</b>	<b>-44.1</b>
$\text{H}_2$	1	-482.7	258.0	48.0
	2	-419.9	297.5	50.2
	3	-413.9	304.9	50.7
	4	-423.3	301.7	50.5
	5	-422.7	301.6	50.5
	6	-422.6	301.9	50.5
	<b>exact</b>	<b>-424.1</b>	<b>301.9</b>	<b>50.5</b>

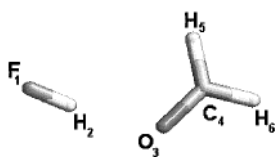
(c)			
coordinate	AIM	DMA	supermolecule
$R(\text{N}_3\text{--H}_2)$	2.127	2.092	1.814
$\angle(\text{N}_3\text{--H}_2\text{--F}_1)$	177.4	180.0	180.0
$\angle(\text{C}_4\text{--N}_3\text{--H}_2)$	153.7	180.0	180.0

AIM both converge to essentially the same geometry at  $L = 6$ , except for two cases where complexes are very floppy.

Our results differ from those of Cooper and Stutchbury<sup>9</sup> because of many possible factors, such as our use of an analytical method<sup>11</sup> to localize minima unambiguously, our higher rank of multipole expansion (feasible by the avoidance of Cartesian tensors), more elaborate basis set and inclusion of correlation. These extra investments offer an overall improvement in the quality of AIM results compared to the supermolecule.

In Table 9 we report the geometry changes in  $\text{HF}\cdots\text{H}_2\text{CO}$  as the rank  $L$  increases. The DMA and AIM models, both at  $L = 6$ , yield very similar angles ( $\angle(\text{C}_4\text{--O}_3\text{--H}_2)$  and  $\angle(\text{C}_4\text{--O}_3\text{--F}_1)$ ). At  $L = 3$  the AIM angles  $\angle(\text{C}_4\text{--O}_3\text{--H}_2)$  and  $\angle(\text{C}_4\text{--O}_3\text{--F}_1)$  are almost  $10^\circ$  smaller than at  $L = 6$  and become very close to the supermolecular angles. This means that a cruder electrostatic picture (i.e.,  $L = 3$  versus  $L = 6$ ) may yield fortuitous agreement with the supermolecule. In other words, to reproduce the supermolecular geometry for the correct reasons the  $L = 6$  picture must be supplemented by interactions omitted in the present work, such as polarization. Extra nonelectrostatic interactions would then correct the purely electrostatic picture and decrease the two aforementioned angles and hence pull the F closer to the H of  $\text{H}_2\text{CO}$ . Note that at the low rank of  $L = 2$ , where only dipole–monopole and dipole–dipole interactions

**TABLE 8: Comparison<sup>a</sup> between DMA and AIM in Terms of (a) the Total Electrostatic Energy  $E_{\text{elec}}(\text{HF}, \text{H}_2\text{CO})$  (kJ/mol), (b) the AIM Atom–Atom Partitioning of the Electrostatic Energy,  $E_{\text{elec}}(\text{A}, \text{B})$ , as a Function of the Multipolar Expansion Rank  $L$ , and (c) the Geometry (Distances in Å and Angles in deg) between the Monomers in  $\text{HF} \cdots \text{H}_2\text{CO}$**



(a)			
	AIM	DMA	
1	−73.0	−19.4	
2	−10.1	−19.1	
3	−21.7	−25.0	
4	−27.2	−25.0	
5	−25.9	−25.4	
6	−25.7	−26.4	
<b>exact</b>	<b>−28.5</b>		

(b)					
	$L$	$\text{O}_3$	$\text{C}_4$	$\text{H}_5$	$\text{H}_6$
$\text{F}_1$	1	342.7	−254.3	−10.4	−7.9
	2	358.9	−294.0	−12.0	−11.7
	3	354.8	−298.2	−12.0	−12.5
	4	355.6	−297.1	−11.9	−12.5
	5	355.2	−296.9	−11.9	−12.4
	6	355.0	−296.8	−11.9	−12.4
	<b>exact</b>	<b>353.9</b>	<b>−296.7</b>	<b>−11.9</b>	<b>−12.4</b>
$\text{H}_2$	1	−492.4	327.0	12.7	9.7
	2	−442.4	361.1	15.6	14.4
	3	−446.1	362.5	14.8	15.0
	4	−451.0	360.0	14.9	14.8
	5	−450.2	360.6	14.9	14.8
	6	−450.0	360.8	14.9	14.8
	<b>exact</b>	<b>−451.9</b>	<b>360.7</b>	<b>14.9</b>	<b>14.8</b>

(c)			
coordinate	AIM	DMA	supermolecule
$R(\text{H}_2-\text{O}_3)$	2.101	2.100	1.696
$\angle(\text{O}_3-\text{H}_2-\text{F}_1)$	171.5	171.3	168.4
$\angle(\text{C}_4-\text{O}_3-\text{H}_2)$	122.7	125.1	113.9
$\angle(\text{C}_4-\text{O}_3-\text{F}_1)$	120.1	122.5	109.8

are allowed, the complex becomes nonplanar within the AIM model, suggesting that its planarity is due to the introduction of the quadrupole interaction at  $L = 3$  in the AIM picture.

Finally an important new point needs to be added to our discussion. An important feature of the DMA approach is that additional sites may be chosen, so as to improve the description of the interaction energy using only lower-rank multipoles.

**TABLE 9: Dependence of the Geometry (Distances in Å and Angles in deg) of  $\text{HF} \cdots \text{H}_2\text{CO}$  on the Total Rank  $L$  in the AIM and DMA Multipole Expansion**

$L$	$R(\text{O}_3-\text{H}_2)^b$		$\angle(\text{O}_3-\text{H}_2-\text{F}_1)$		$\angle(\text{C}_4-\text{O}_3-\text{H}_2)$		$\angle(\text{C}_4-\text{O}_3-\text{F}_1)$	
	AIM	DMA	AIM	DMA	AIM	DMA	AIM	DMA
1	2.073	2.102	180.0	180.0	180.0	180.0	180.0	180.0
2	2.146 <sup>a</sup>	2.100	161.4	180.0	129.4	180.0	123.9	180.0
3	2.127	2.100	162.9	173.1	116.1	133.2	111.0	131.0
4	2.099	2.103	171.4	171.2	125.3	131.9	122.7	129.2
5	2.101	2.098	171.2	173.4	125.3	122.3	122.6	120.2
6	2.101	2.100	171.5	171.3	122.7	125.1	120.1	122.5

<sup>a</sup> The complex is planar for all entries except here where the dihedral angle  $\text{H}_2-\text{O}_3-\text{C}_4-\text{H}_5$  is  $89.9^\circ$ . <sup>b</sup> The labels refer to the same labeling scheme as in Table 8.

Current research<sup>30</sup> shows it is possible to introduce extra sites inside the atomic basin, without fundamentally changing the AIM multipole moments. Hence it is possible to accelerate the convergence of the AIM multipole expansion without losing the advantage of a rigorous atomic partitioning. One should bear in mind that a correct comparison between the convergence behavior of DMA and AIM can only happen with an equal number of sites.

## 5. Conclusion

We have proposed an atom–atom partitioning of the electrostatic interaction based on the topology of the electron density (AIM) and the compact multipole moments introduced by the spherical tensor formalism. We were interested in a *careful* test of this proposal in the context of the successful Buckingham–Fowler model, using improved algorithms. Particular attention was paid to the convergence of both the energy and the geometry of a set of van der Waals complexes, with respect to the rank  $L$  of the multipole expansion. For the first time this convergence behavior has been contrasted with exact values, obtained without multipole expansion, via 6D integration over two atomic basins. We find that, although the AIM results converge more slowly than the DMA results, excellent agreement is obtained between the two methods at high rank ( $L = 6$ ), for both geometry as well as intermolecular electrostatic interaction energy. This is the first time that a direct, complete, and explicit comparison between AIM and DMA has been made. Contrary to views expressed before in the literature, this work opens an avenue to introduce the topological approach in the construction of an accurate intermolecular force field. It is here that the high degree of transferability of the functional groups defined by AIM will be extremely useful.

**Acknowledgment.** Gratitude is expressed to EPSRC who sponsors this work via grant GR/M18119.

## Appendix

**Derivation of Multipolar Expansion of Electrostatic Interaction between Topological Atoms.** In Figure 1 two interacting atomic basins  $\Omega_A$  and  $\Omega_B$  are shown, each centered on a nucleus with coordinates  $\mathbf{R}_A$  and  $\mathbf{R}_B$ , respectively. Note that  $\mathbf{R}_A$  and  $\mathbf{R}_B$  are expressed with respect to a common lab frame with origin  $\mathbf{o}$ . The charge density within  $\Omega_A$  ( $\Omega_B$ ) is described by the position vector  $\mathbf{r}_A$  ( $\mathbf{r}_B$ ), which is centered on the respective nucleus. For the practical computation of the electrostatic energy we ensure that both molecular charge densities are referred to a common global frame. Hence, the position vector of an infinitesimal charge element in  $\Omega_A$  is  $\mathbf{R}_A + \mathbf{r}_A$ , and  $\mathbf{R}_B + \mathbf{r}_B$  for an element in  $\Omega_B$ . The electrostatic interaction between two infinitesimal charge elements, one in

each atom, contains  $|\mathbf{r}_1 - \mathbf{r}_2| = |\mathbf{r}_{AB}|$  where  $\mathbf{r}_{AB} = (\mathbf{R}_B + \mathbf{r}_B) - (\mathbf{R}_A + \mathbf{r}_A) = \mathbf{R}_{AB} - (\mathbf{r}_A - \mathbf{r}_B)$ .

Substituting eq 2 into eq 3 (main text) we obtain for the exact electrostatic energy between atoms A and B:

$$E_{\text{elec}}(A,B) = \int_{\Omega_A} d\mathbf{r}_A \int_{\Omega_B} d\mathbf{r}_B \frac{\rho_{\text{tot}}(M_A; \mathbf{r}_A) \rho_{\text{tot}}(M_B; \mathbf{r}_B)}{|\mathbf{R}_{AB} - (\mathbf{r}_A - \mathbf{r}_B)|} \\ = \int_{\Omega_A} d\mathbf{r}_A \rho_{\text{tot}}(M_A; \mathbf{r}_A) V_B(\mathbf{r}_A) = Z_A V_B(\mathbf{R}_A) - \int_{\Omega_A} d\mathbf{r}_A \rho(M_A; \mathbf{r}_A) V_B(\mathbf{r}_A) \quad (\text{A1})$$

where  $V_B(\mathbf{r}_A) = \int_{\Omega_B} d\mathbf{r}_B \rho_{\text{tot}}(M_B; \mathbf{r}_B) / |\mathbf{R}_{AB} - (\mathbf{r}_A - \mathbf{r}_B)|$  is the electrostatic potential generated by atom B in atom A.

The direct integration over two atomic basins is a feasible but rather expensive calculation. To make substantial CPU time savings we introduce multipole moments in analogy with the computation of the electrostatic interaction in large monomer clusters.

Following Stone (ref 13, pp 41–43) we now derive in a self-contained but concise way the expansion of the electrostatic interaction energy in terms of spherical multipole moments (eq 5 of the main text). A binomial Taylor expansion of the expression  $|\mathbf{R}_{AB} - (\mathbf{r}_A - \mathbf{r}_B)|^{-1}$  factors the electronic  $(\mathbf{r}_A, \mathbf{r}_B)$  and geometric  $(\mathbf{R}_{AB})$  coordinates as follows;<sup>31</sup>

$$\frac{1}{|\mathbf{R}_{AB} - (\mathbf{r}_A - \mathbf{r}_B)|} = \sum_{l=0}^{\infty} \sum_{m=-l}^l (-1)^m R_{l,-m}(\mathbf{r}_A - \mathbf{r}_B) I_{l,m}(\mathbf{R}_{AB}) \quad (\text{A2})$$

where  $R_{lm}(\mathbf{r}_A - \mathbf{r}_B)$  and  $I_{lm}(\mathbf{R}_{AB})$  are the regular and irregular normalized spherical harmonics  $Y_{lm}(\theta, \varphi)$ , respectively:

$$R_{l,m}(\mathbf{r}) = \sqrt{\frac{4\pi}{2l+1}} r^l Y_{l,m}(\theta, \varphi) \quad (\text{A3a})$$

$$I_{l,m}(\mathbf{r}) = \sqrt{\frac{4\pi}{2l+1}} r^{-l-1} Y_{l,m}(\theta, \varphi) \quad (\text{A3b})$$

This expansion *formally* converges provided  $|\mathbf{r}_A - \mathbf{r}_B| < |\mathbf{R}_{AB}| = \mathbf{R}_{AB}$ . In other words if the atomic basins are small compared to the internuclear distance  $\mathbf{R}_{AB}$ , then the convergence criterion will be obeyed. This convergence criterion is typically violated if the relative orientation and size of the atomic basins is such that two long and oppositely directed vectors  $\mathbf{r}_A$  and  $\mathbf{r}_B$  arise.

Using an addition theorem for regular spherical harmonics,<sup>31</sup> we can again factorize  $R_{l,-m}(\mathbf{r}_A - \mathbf{r}_B)$ , leading to a convenient expansion of  $|\mathbf{R}_{AB} - (\mathbf{r}_A - \mathbf{r}_B)|^{-1}$  in terms of three separate coordinates  $\mathbf{R}_{AB}$ ,  $\mathbf{r}_A$ , and  $\mathbf{r}_B$ :

$$\frac{1}{|\mathbf{R}_{AB} - (\mathbf{r}_A - \mathbf{r}_B)|} = \sum_{l_A=0}^{\infty} \sum_{l_B=0}^{\infty} \sum_{m_A=-l_A}^{l_A} \sum_{m_B=-l_B}^{l_B} T_{l_A l_B m_A m_B}(\mathbf{R}_{AB}) R_{l_A m_A}(\mathbf{r}_A) R_{l_B m_B}(\mathbf{r}_B) \quad (\text{A4})$$

and

$$T_{l_A l_B m_A m_B}^{(G)}(\mathbf{R}_{AB}) = (-1)^{l_A} \sqrt{\frac{(2l_A + 2l_B + 1)!}{(2l_A)!(2l_B)!}} \\ \begin{pmatrix} l_A & l_B & l_A + l_B \\ m_A & m_B & -(m_A + m_B) \end{pmatrix} I_{l_A + l_B, -(m_A + m_B)}(\mathbf{R}_{AB}) \quad (\text{A5})$$

where the expression in large brackets is a Wigner 3j symbol<sup>31</sup> and the superscript (G) reminds us everything is defined with respect to one common global frame.

Substituting eq A4 into the defining equation, main eq 3 (realizing that  $|\mathbf{r}_1 - \mathbf{r}_2| = |\mathbf{R}_{AB} - (\mathbf{r}_A - \mathbf{r}_B)|$ ) leads to:

$$E_{\text{elec}}(A,B) = \sum_{l_A l_B m_A m_B} T_{l_A l_B m_A m_B}^{(G)}(\mathbf{R}_{AB}) \int_{\Omega_A} d\mathbf{r}_A \rho_{\text{tot}}(M_A; \mathbf{r}_A) \times \\ R_{l_A m_A}(\mathbf{r}_A) \int_{\Omega_B} d\mathbf{r}_B \rho_{\text{tot}}(M_B; \mathbf{r}_B) R_{l_B m_B}(\mathbf{r}_B) \\ = \sum_{l_A l_B m_A m_B} T_{l_A l_B m_A m_B}^{(G)}(\mathbf{R}_{AB}) Q_{l_A m_A}^{(G)}(\Omega_A) Q_{l_B m_B}^{(G)}(\Omega_B) \quad (\text{A6})$$

where  $T_{l_A l_B m_A m_B}^{(G)}$  is a purely geometric interaction tensor and  $Q_{lm}^{(G)}$  are the  $2l + 1$  multipole moments of rank  $l$  with respect to the global frame. With an eye on eq A3b, we can appropriately group the terms in eq A6 according to the power of the interaction distance  $\mathbf{R}_{AB}^{-(l_A + l_B + 1)} = \mathbf{R}_{AB}^{-L}$ . In other words, by defining  $L$  as  $l_A + l_B + 1$  we collect interaction terms that have the same  $\mathbf{R}$ -dependence. For example, for  $L = 3$  the only possible combinations are  $l_A = 0, l_B = 2$ ;  $l_A = 1, l_B = 1$ ; and  $l_A = 2, l_B = 0$ , which correspond to the monopole–quadrupole, dipole–dipole and quadrupole–monopole interactions, respectively.

Equation A6 is not convenient for direct use because the multipole moments of isolated monomers are computed in a *local* frame that has an arbitrary orientation with respect to the global frame. The moments in the local frame are related to those of the global frame by

$$Q_{lm}^{(G)} = \sum_k Q_{lk}^{(L)} [D_{mk}^{(L)}(\alpha, \beta, \gamma)]^* \quad (\text{A7})$$

where  $(\alpha, \beta, \gamma)$  is the rotation that takes the global axes to the local axes and  $[D_{mk}^{(L)}]^*$  is the conjugate of the Wigner rotation matrix.<sup>13</sup> Substituting eq A7 into eq A6 and rearranging yields

$$E_{\text{elec}}(A,B) = \sum_{l_A l_B k_A k_B} T_{l_A l_B k_A k_B}^{(L)}(\mathbf{R}_{AB}) Q_{l_A k_A}^{(L)}(\Omega_A) Q_{l_B k_B}^{(L)}(\Omega_B) \quad (\text{A8})$$

where the “local” interaction tensor  $T^{(L)}$  is related to the “global” one via

$$T_{l_A l_B k_A k_B}^{(L)}(\mathbf{R}_{AB}) = \sum_{l_A' l_B' k_A' k_B'} T_{l_A' l_B' k_A' k_B'}^{(G)}(\mathbf{R}_{AB}) [D_{m_A k_A}^{(L)}]^* [D_{m_B k_B}^{(L)}]^* \quad (\text{A9})$$

Explicit formulas for interaction tensors in the general case have been published before<sup>13</sup> for  $L \leq 5$  or  $l_A + l_B \leq 4$ , while Hättig and Hess<sup>32</sup> also listed explicit formulas for  $L = 6$  or  $l_A + l_B = 5$ .

Finally, since  $Y_{lm}(\theta, \varphi)$  is complex if  $m \neq 0$ , the moments  $Q_{lm}$  can be complex. It is convenient to work with real multipole moments, which can be introduced by taking suitable linear combinations.<sup>13</sup> Real AIM spherical tensor multipole moments were defined before<sup>14</sup> and also used in our work on the electrostatic potential.<sup>33,34</sup>

## References and Notes

- (1) Fowler, P. W.; Buckingham, A. D. *Mol. Phys.* **1983**, *50*, 1349.
- (2) Buckingham, A. D.; Fowler, P. W. *Can. J. Chem.* **1985**, *63*, 2018.
- (3) Stone, A. J. *Chem. Phys. Lett.* **1981**, *83*, 233.
- (4) Price, S. L. *Rev. Comput. Chem.* **2000**, *14*, 225.
- (5) Nobeli, I.; Price, S. L. *J. Phys. Chem. A* **1999**, *103*, 6448.



- (6) Bader, R. F. W. *Atoms in Molecules. A Quantum Theory*; Oxford University Press: Oxford, 1990.
- (7) Popelier, P. L. A. *Atoms in Molecules. An Introduction*. Pearson Education: Harlow, UK, 2000.
- (8) Popelier, P. L. A.; Aicken, F. M.; O'Brien, S. E. *Atoms in Molecules*; Hinchliffe, A., Ed.; Royal Society of Chemistry: 2000; Vol. 1, pp 143–198.
- (9) Cooper, D. L.; Stutchbury, N. C. J. *Chem. Phys. Lett.* **1985**, *120*, 167.
- (10) Stone, A. J.; Alderton, M. *Mol. Phys.* **1985**, *56*, 1047.
- (11) Popelier, P. L. A.; Stone, A. J. *Mol. Phys.* **1994**, *82*, 411.
- (12) Popelier, P. L. A.; Stone, A. J.; Wales, D. J. *Faraday Discuss.* **1994**, *97*, 243.
- (13) Stone, A. J. *The theory of intermolecular forces*; Clarendon: Oxford, 1996.
- (14) Popelier, P. L. A. *Mol. Phys.* **1996**, *87*, 1169.
- (15) Popelier, P. L. A. *Comput. Phys. Commun.* **1998**, *108*, 180.
- (16) Wheatley, R. J. *Mol. Phys.* **1995**, *86*, 443.
- (17) Popelier, P. L. A.; Kosov, D. S. *J. Chem. Phys.* **2001**, *114*, 6539.
- (18) Freitag, M. A.; Gordon, M. S.; Jensen, J. H.; Stevens, W. J. *J. Chem. Phys.* **2000**, *112*, 7300.
- (19) Frisch, M. J.; Trucks, G. W.; Schlegel, H. B.; Scuseria, G. E.; Robb, M. A.; Cheeseman, J. R.; Zakrzewski, V. G.; Montgomery, J. A., Jr.; Stratmann, R. E.; Burant, J. C.; Dapprich, S.; Millam, J. M.; Daniels, A. D.; Kudin, K. N.; Strain, M. C.; Farkas, O.; Tomasi, J.; Barone, V.; Cossi, M.; Cammi, R.; Mennucci, B.; Pomelli, C.; Adamo, C.; Clifford, S.; Ochterski, J.; Petersson, G. A.; Ayala, P. Y.; Cui, Q.; Morokuma, K.; Malick, D. K.; Rabuck, A. D.; Raghavachari, K.; Foresman, J. B.; Cioslowski, J.; Ortiz, J. V.; Stefanov, B. B.; Liu, G.; Liashenko, A.; Piskorz, P.; Komaromi, I.; Gomperts, R.; Martin, R. L.; Fox, D. J.; Keith, T.; Al-Laham, M. A.; Peng, C. Y.; Nanayakkara, A.; Gonzalez, C.; Challacombe, M.; Gill, P. M. W.; Johnson, B. G.; Chen, W.; Wong, M. W.; Andres, J. L.; Head-Gordon, M.; Replogle, E. S.; Pople, J. A. *Gaussian 98, revision A.7*; Gaussian, Inc.: Pittsburgh, PA, 1998.
- (20) Krishnan, R.; Binkley, J. S.; Seeger, R.; Pople, J. A. *J. Chem. Phys.* **1980**, *72*, 650.
- (21) Becke, A. D. *J. Chem. Phys.* **1993**, *98*, 5648.
- (22) O'Brien, S. E.; Popelier, P. L. A. *Can. J. of Chem.* **1999**, *77*, 28.
- (23) Foresman, J. B.; Frisch, A. *Exploring Chemistry with Electronic Structure Methods*; 2nd ed.; Gaussian Inc.: Pittsburgh, 1996.
- (24) MORPHY01 a program written by P. L. A. Popelier with a contribution from R. G. A. Bone, D. Kosov, M. in het Panhuis, UMIST, Manchester, England, EU 2001.
- (25) Aicken, F. M.; Popelier, P. L. A. *Can. J. of Chem.* **2000**, *78*, 415.
- (26) Stone, A. J.; Dullweber, A.; Hodges, M. P.; Popelier, P. L. A.; Wales, D. J. *ORIENT 3.2j*; Cambridge, 1996.
- (27) Bondi, A. J. *Phys. Chem.* **1964**, *68*, 441.
- (28) Pauling, L. *The Nature of the Chemical Bond*, 3rd ed.; Cornell University Press: Ithaca, NY, 1960.
- (29) Cornell, W. D.; Chipot, C. *Encyclopedia of Computational Chemistry*; Schleyer, P. v. R., Ed.; Wiley: New York, 1998; Vol. 1, p 258.
- (30) Joubert, L.; Popelier, P. L. A., unpublished results, 2001.
- (31) Varshalovich, D. A.; Moskalev, A. N.; Khersonskii, V. K. *Theory of angular momentum*; World Scientific: River Edge, NJ, 1988.
- (32) Hättig, C.; Hess, B. A. *Mol. Phys.* **1994**, *81*, 813.
- (33) Kosov, D. S.; Popelier, P. L. A. *J. Chem. Phys.* **2000**, *113*, 3969.
- (34) Kosov, D. S.; Popelier, P. L. A. *J. Phys. Chem. A* **2000**, *104*, 7339.